ILMATIETEEN LAITOS
METEOROLOGISKA INSTITUTET
FINNISH METEOROLOGICAL INSTITUTE

HELSINGIN YLIOPISTO
HELSINGFORS UNIVERSITET
UNIVERSITY OF HELSINKI

SLSTR/AATSR VIEWING GEOMETRY SIMULATED WITH MISR

Timo H. Virtanen[1,*], Pekka Kolmonen[1], Larisa Sogacheva[1], Edith Rodriguez[1], and Gerrit de Leeuw[1,2]

[1]Finnish Meteorological Institute, Helsinki, Finland, [2]Department of Physics, University of Helsinki, Finland, *Email: timo.h.virtanen@fmi.fi

Introduction

In this poster the effects of the satellite viewing geometry to the ADV aerosol retrieval algorithm are studied. The AATSR Dual View (ADV) aerosol retrieval algorithm used at FMI is based on the stereo-viewing capability of AATSR. ADV uses the k-ratio approach, in which the radiances measured in nadir and forward views are used to eliminate the surface reflectance contribution from the top of atmosphere (TOA) reflectance, allowing us to retrieve the aerosol contribution without any prior knowledge of the surface properties.

In preparation for he use of ADV with SLSTR data, the changing oblique viewing direction from a forward view in AATSR to a backward view in SLSTR needs to be addressed. Here we use the MISR data to study the effects of the viewing geometry prior to the launch of Sentinel-3.

Viewing geometry

The ADV aerosol retrieval algorithm is based on the dual view capability of AATSR and SLSTR. In principle the algorithm can handle any viewing geometry, but in practice there can be differences in the performance for different viewing geometries. Both the aerosol optical properties (phase function) and the surface properties (BRDF) affect the observed TOA signal, and depend on the viewing geometry.

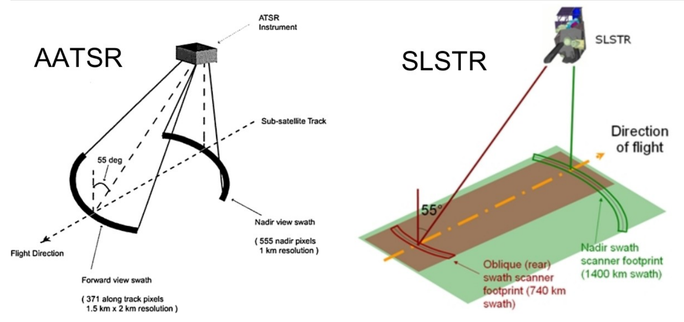

Figure 1. Schematics of the AATSR and SLSTR viewing geometry. (Credits: ESA, AATSR Handbook 2007; Donlon et al. 2012.)

Instrument specifics

	SLSTR	AATSR	MISR
Swath	1420 km (nadir) 750 km (backwards)	500 km	360 km
Global coverage (at the equator)	2 days (nadir) 4 days (backwards)	6 days	9 days
Resolution	0.5 km (VIS-SWIR) 1 km (IR)	1 km	275 m (nadir and red) 1.1 km (other)
Channels (μm):	0.555, 0.659, 0.865 **1.375**, 1.61, **2.25** 3.74, 10.85, 12	0.555, 0.659, 0.865 1,61 3.74, 10.85, 12	0.446, 0.558, 0.672, 0.867
Data per orbit	20 GB	0.8 GB	2.3 GB
Oblique view	Backward 55º	Forward 55º	26.1º, 45.6º, 60.0º, 70.5º

Table 1: Comparison of the AATSR, SLSTR and MISR characteristics[1,2,3]. The differences most relevant to aerosol retrievals are: **(1)** Two new channels: 1.375 μm and 2.25 μm. **(2)** Larger swath: ∼740 km for dual view, and ∼1400 km for nadir view, compared to 500 km of AATSR. **(3)** Increased resolution: 0.5 km for VIS-SWIR. **(4)** The oblique view is in the backward direction instead of forward.

ADV principles

The ADV algorithm uses the k-ratio approach to eliminate surface reflectance from the retrieval equations[4,6]. In ADV the k-ratio (ratio of the oblique and nadir view surface reflectance) is assumed independent of wavelength, and approximated (initially) by the TOA reflectance at 1.6 μm. Once the surface contribution has been eliminated from the TOA reflectance, the aerosol model which best describes the remaining path radiance is selected in ADV by minimizing the difference between the observed and modeled reflectance, using the 0.555, 0.659 and 1.6 μm wavelengths. After the AOD retrieval the aerosol contribution can be subtracted from the TOA signal to obtain the surface reflectance[5].

To study the possible effects of the changing viewing geometry prior to the launch of Sentinel-3, we use MISR data. In addition to the MISR nadir view camera (AN), We use the 60° forward (CF), and 60° backward (CA) cameras, respectively. Unfortunately, MISR lacks the 1.6 μm channel which is crucial in ADV, but nonetheless we can run ADV in a special two-wavelength (2wl) mode with MISR data. This limited 2wl mode is not expected to give very accurate information on the aerosol loads, but it can still be useful in studying the performance of the algorithm in different viewing geometries.

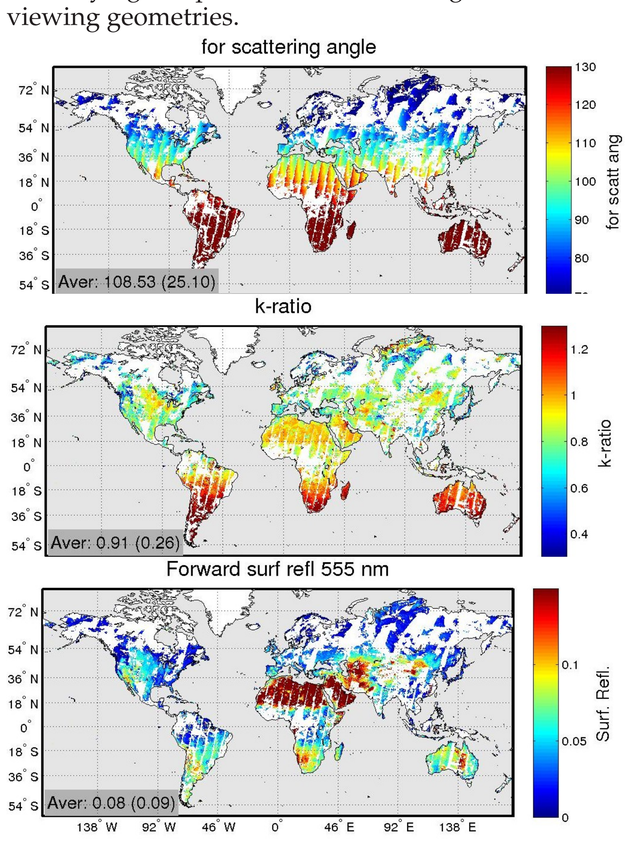

Figure 2. Global maps of scattering angle, k-ratio, and surface reflectance for AATSR on September 2008.

Results

Here we compare results obtained by using ADV with MISR forward and backward data, respectively.

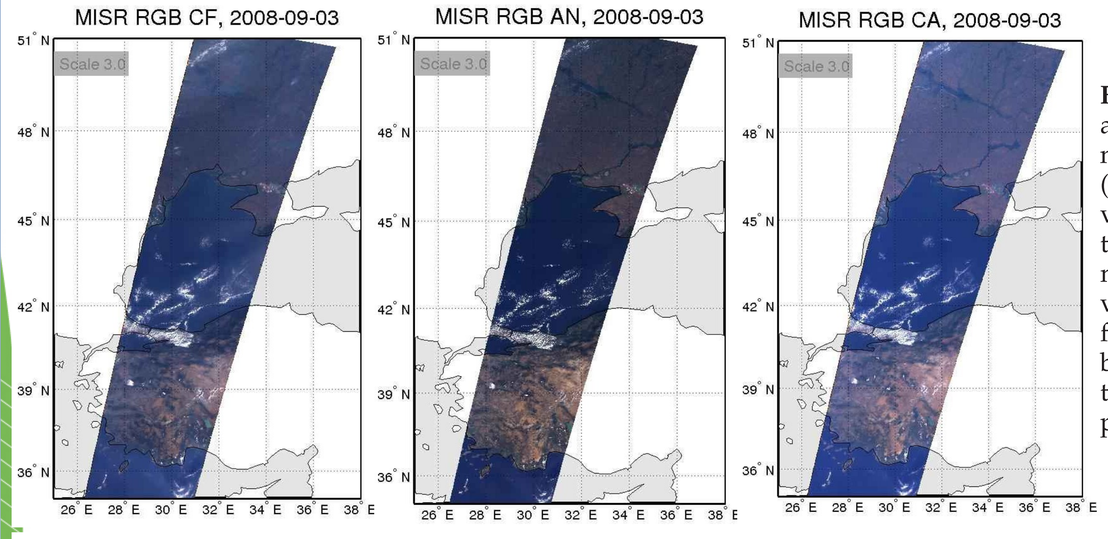

Figure 3. MISR RGB images for the forward (CF), nadir (AN) and backward (CA) views. Both oblique views appear hazy due to larger aerosol signal - more so for the backward view. The surface reflectance is highest for the backward view: more detail is seen on the northern part of the scene.

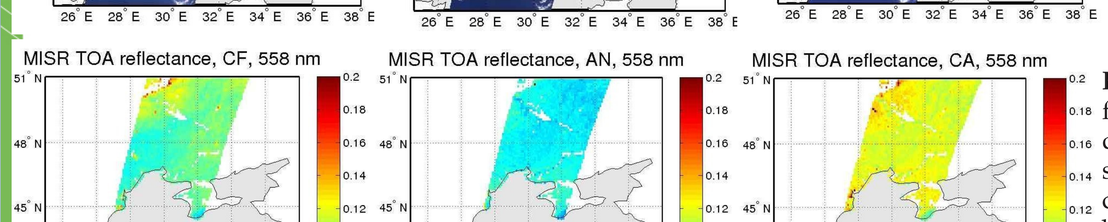

Figure 4. MISR TOA reflectance at 558 nm for different views. For this scene the reflectance is clearly highest for the backward view. This is typical for the northern hemisphere (NH). For the southern hemisphere (SH) the opposite is true (see Fig. 2c).

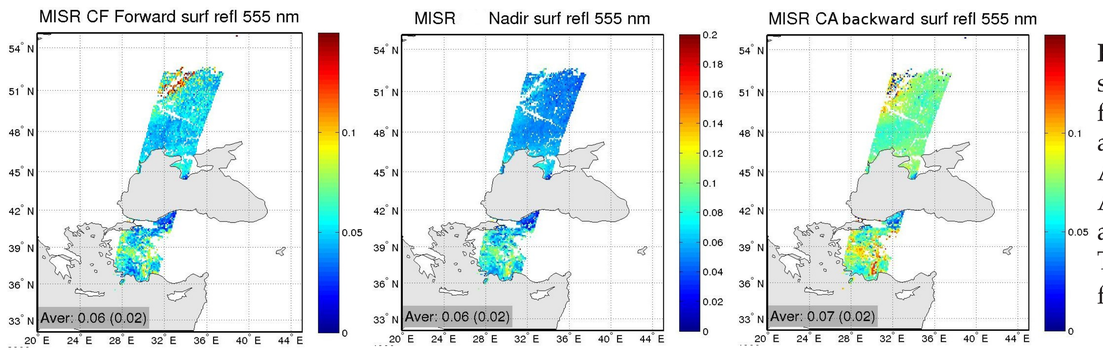

Figure 5. The ADV-retrieved surface reflectance for MISR forward (CF), nadir (AN), and backward (CA) views. After the AOD retrieval in ADV we can reduce the aerosol reflectance from the TOA signal to obtain the surface reflectance[5].

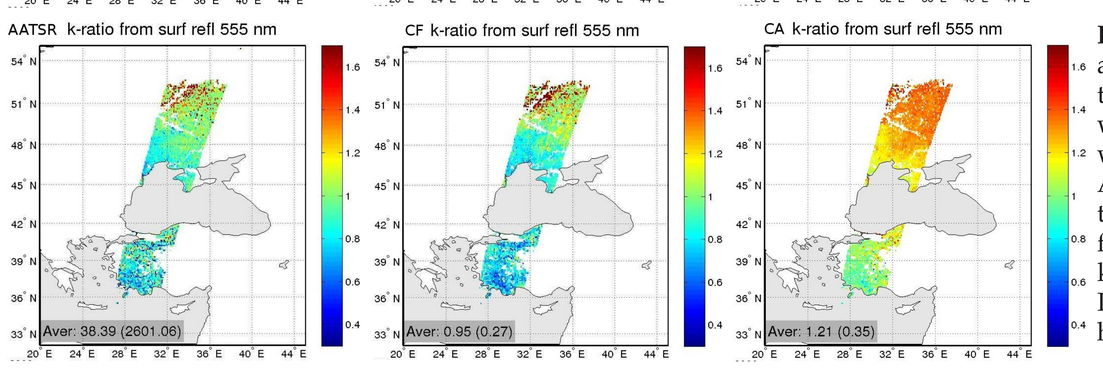

Figure 6. Surface k-ratio after surface reflectance retrieval for AATSR, MISR forward (CF), and MISR backward (CA) views. For AATSR and MISR forward the results are similar, but for MISR backward view the k-ratios are higher in NH. In SH the forward view has higher k-ratios.

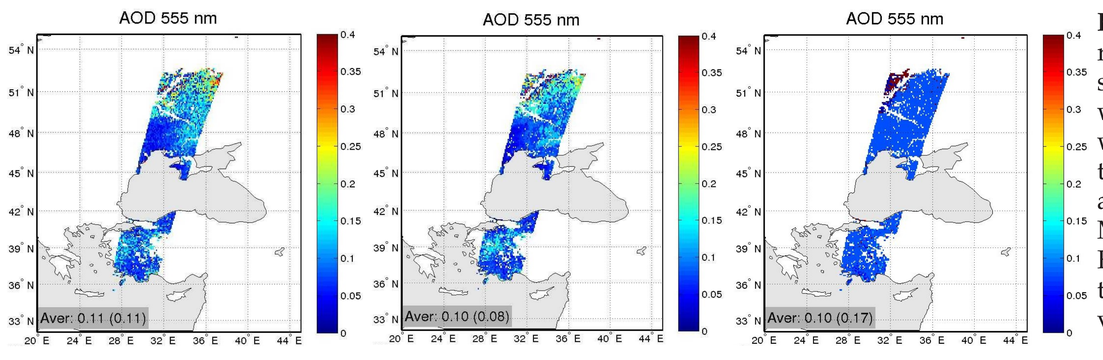

Figure 7. Preliminary AOD retrieval with ADV-2wl version for AATSR, MISR forward view, and MISR backward view. The qualitative results show that results agree for the AATSR and MISR forward view data. For MISR backward view the retrieval does not converge properly.

References

[1] Diner, D.J, C.J. Bruegge, J.V. Martonchik, T.P. Ackerman, R. Davies, S.A.W. Gerstl, H.R. Gordon, P.J. Sellers, and J. Clark, J.A. Daniels, E.D. Danielson, V.G. Duval, K.P. Klassen, G.W. Lilienthal, D.I. Nakamoto, R. Pagano, T.H. Reilly, MISR: A Multi-angle Imaging SpectroRadiometer for geophysical and climatological research from EOS. IEEE TGRS, 27 (2), 200-214, 1989.

[2] Donlon, C., Berruti, B., Buongiorno, A., Ferreira, M.-H., Féménias, P., Frerick, J., Goryl, P., Klein, U., Laur, H., Mavrocordatos, C., Nieke, J., Rebhan, H., Seitz, B., Stroede, J., Sciarra, R, The Global Monitoring for Environment and Security (GMES) Sentinel-3 Mission, RSE, 120, 27-57, 2012.

[3] ESA, Sentinel-3: ESA's Global Land and Ocean Mission for GMES Operational Services, ESA SP-1322/3, October 2012.

[4] Flowerdew, R.J. and Haigh, J.D., An approximation to improve accuracy in the derivation of surface reflectances from multi-look satellite radiometers, GRL, 22 1693-1696, 1995.

[5] Sogacheva, L., Kolmonen, P., Virtanen, T. H., Rodriguez, E., Sundström, A.-M., and de Leeuw, G.: Determination of land surface reflectance using the AATSR dual-view capability, AMT, 8, 891-906, 2015.

[6] Veefkind, J.P., de Leeuw, G.D., and Durkee, P.A., Retrieval of aerosol optical depth over land using two-angle view satellite radiometry during TARFOX, GRL, 25 3135-3138, 1999.